Charge reorganization at the adsorbate covered electrode surface probed through in-situ resonant x-ray diffraction combined with ab initio modelling

Yvonne Grunder, Christopher Lucas, Paul Thompson, Yves Joly, Y. Soldo

Charge reorganization at the adsorbate covered electrode surface probed through in-situ resonant x-ray diffraction combined with *ab initio* modelling

Yvonne Grunder,[‡,] * Christopher A. Lucas,[‡] Paul B.J. Thompson,[‡,†] Yves Joly,[§] Yvonne Soldo-Olivier[§]

[‡] Oliver Lodge Laboratory, Department of Physics, University of Liverpool, Liverpool L69 72E, UK

[†] XMaS Beamline, European Synchrotron Radiation Facility, F-38043 Grenoble, France

[§] Université Grenoble Alpes, CNRS, Institut Néel, 38042 Grenoble, France

KEYWORDS bond formation, electrochemical interface, interfacial charge, ab-initio calculation, in-situ characterization, x-ray diffraction

ABSTRACT: Understanding the charge distribution and bonding mechanism at the polarized solid-liquid interface is a fundamental challenge in electrochemistry which impacts on applications ranging from materials processing to renewable energy production. The applied potential, ions in solution and the polarization of the interface all combine to alter the bond formation and the interfacial charge distribution thus techniques must be developed to provide in-situ characterization of the interface. Here we present a combination of in-situ resonant surface x-ray diffraction studies and self-consistent DFT calculations to assess the charge distribution and bonding mechanism for the adsorption of bromide anions onto a single crystal Cu(001) electrode surface. Comparison between the experimental and modelled data gives detailed information about the charge distribution at the interface and the bonding of specific adsorbates, predicting a charge rearrangement rather than charging of the atoms involved and a surface dipole moment situated at the metal surface.

1. Introduction

Although electrochemical interfaces play a key role in many day-to day applications ranging from renewable energy production to materials processing, detailed information on the charge distribution at the interface and its influence on reactivity, activity and phase formation is not easy to obtain. Understanding the influence of the applied electrochemical potential, the interfacial atomic arrangement and adsorbate layer formation on the nature of the charge transfer and the interfacial electronic structure is central to developing a fundamental understanding of electrochemical reactions. Adsorbates play a crucial role in electrochemical processes such as phase formation during electrodeposition[1-4] and during electrocatalytic reactions[5], where they can be present at the interface either as adsorbed species from the electrolyte solution or as reaction intermediates. Adsorbates can also affect the electrode stability and result in degradation of the electrode.[6-10] Insights into the exact mechanism of adsorbate bonding at the electrochemical interface, the polarizability of the bond and its dependence on the applied potential will thus help to better understand and design electrochemical processes. In addition, insight into bond formation and modification by surrounding ions or an electrical field is of more general interest to several areas in Chemistry, such as bio-molecular or complex-formation .[11-12]

Although recent advances have been made in understanding the atomic scale structure of the electrode–electrolyte interface and helped to elucidate many interfacial electrochemical phenomena, including the ion arrangements close to the electrode surface,[13-19] the exact nature of the charge distribution at the electrochemical interface is not understood. The distribution of charges in the absence and presence of adsorbates has been extensively discussed in terms of partial charge transfer and electrosorption valencies, but up to now without direct measurements of these parameters.[20-23] The situation is complicated by the phenomenon of non-specific adsorption which can alter the potential distribution at the interface. The effect of the double layer structure and composition on catalytic reactions has been suggested and recognized for a number of examples,[24-29] but the exact effect on the charge distribution is difficult to probe experimentally. Possible indications about the electron density and potential drop modification near the electrode surface in the presence of chemisorbed adsorbates by non-specifically adsorbed ions can be gained from molecular dynamics simulations, whereas the near range ordering of the ions in solution is accessible through x-ray reflectivity and surface x-ray scattering.[14, 30-31] Experimental verification of the theoretical results from molecular dynamics simulations, such as a direct probing of the predicted electron density and modification by the applied potential and electrolyte ordering is still lacking.

Due to the buried nature of the electrochemical interface standard electron spectroscopy techniques which could give details about interfacial electron densities are difficult to employ, although there has been progress recently in developing ambient pressure photoelectron spectroscopy, despite the rather severe experimental limitations required for the technique to be feasible.[32] Resonant surface x-ray diffraction has been employed previously to study oxidation state changes during the anodic oxidation of Pt(111) electrodes and to probe the adsorption of carbon monoxide onto the Pt electrode surface.[33-34] First principles calculations were made to reproduce the essential features in the signal from the specularly reflected x-rays and the modelling was restricted to the forward scattering cross sections, only allowing a qualitative comparison with the experimental data. The authors laid out the necessary computational steps to be taken for a more quantitative analysis of the x-ray diffraction data. Recently we have managed to successfully implement these computational steps into the FDMNES program[35-36] to allow the first-principles simulation of resonant surface x-ray diffraction data.[37-38] In this paper we present experimental measurements and first principles calculations of the resonant surface x-ray diffraction from a bromide-covered Cu(001) electrode in the electrochemical environment. As shown in previous measurements[39] this system is an ideal test case to develop the methodologies as the c(2x2) ordering of the bromide adlayer enables specific bromide and Cu atoms to be selected by the diffraction conditions for the spectroscopic measurements. Each resonant diffraction spectra measured at a position in reciprocal space has a distinguished contribution from the surface and the bulk atoms. The x-ray scattering amplitude depends on the electron density of the contributing atoms and thus any modification of charge distribution should be observable in a modification of the scattered intensity close to the adsorption edge of the specific atom.[40] The intensity variation at each position in reciprocal space is thus specific to the spectroscopic response of the atoms contributing to the intensity at that specific positions and to the modification of the atomic form factor due to the change in the electron arrangement at the interface. The effect of the electrochemical potential drop and the near interfacial ions were not included in previous calculations.[37] These effects can modify the electron density of the surface atoms and subsequently the resonant diffraction signal close to the absorption edge. Here we mimic the electrochemical environment by including the effect of a simple double layer model at the electrochemical interface and this has been implemented into the FDMNES code. The results yield new insights into the underlying bonding and charge distribution, suggesting a charge rearrangement and a surface dipole moment situated at the metal surface.

2. Methodology

2.1 Theoretical details

The modelling of the data extends our recent developments of the FDMNES code to model resonant surface x-ray diffraction data[37] by including the effect of the electrochemical interface and applied potential in the form of a Helmholtz potential due to the double layer and ions present at the interface. To account for the electrochemical double layer, we included an additional potential V_{Helm} as would be expected from a three-dimensional Gaussian charge distribution $\rho(z)=\frac{\rho_0}{\sqrt{(2\pi)^3\sigma^3}}\exp(-\frac{(z-z_0)^2}{2\sigma^2})$ at a distance z_0 from the surface, with a width σ and containing the total charge ρ_0. The additional potential V_{Helm} then takes the form of a peak centered at z_0 and described by the relationship: $V_{Helm}(z)=V_0\frac{\sqrt{\pi}}{2}\frac{\mathrm{erf}(\frac{(z-z_0)}{\sqrt{2}\sigma})}{\frac{(z-z_0)}{\sqrt{2}\sigma}}$, where $\sigma=\frac{\alpha\,\Delta H}{\sqrt{2}}$ with α=0.285925 is linearly related to ΔH, the FWHM of the potential. This potential accounts for the counter ions plane present close to the interface. The potential is schematically shown together with the surface atomic positions in Figure 1 for the particular system under study, namely bromide anions adsorbed onto a Cu(001) electrode surface. This model is necessary to account for the ion accumulation at the interface and the resulting electrostatic potential, induced by the applied electrochemical potential and the electrolyte.

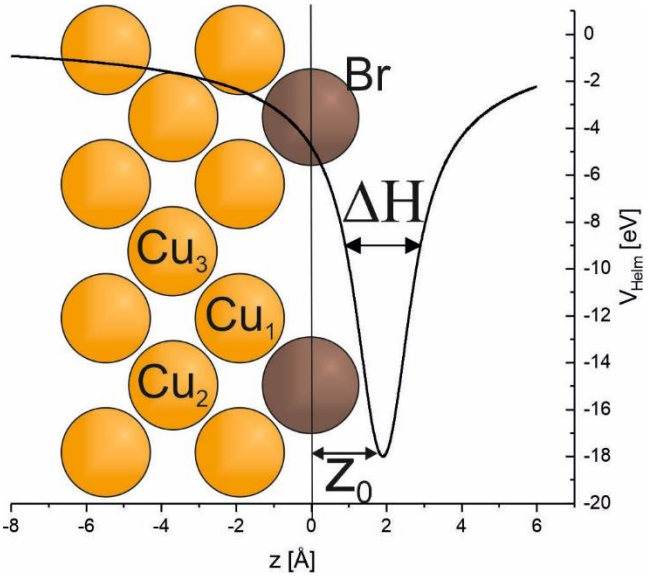

Figure 1. The Helmholtz potential $V_{Helm}(z)$ is depicted together with the positions of the surface atoms. The different copper atoms (orange) and the bromine atoms (brown) sites are labelled, with Cu_1 referring to the Cu in the 1st atomic layer, Cu_2 and Cu_3 referring to the Cu atom in the second atomic layer to a position below the Br atom and to a position without a Br atom on top, respectively. The adjustable parameters of the potential are ΔH, the FWHM of the potential V_{helm}, the distance z_0 of the center of the charge layer from the surface and V_0 the maximum value of the potential.

Note that this is a simplistic model to represent a possible counter charge close to the electrode surface and does not necessary represent the 'real' form of the induced potential modification. This work is aiming to elucidate the change of the charge distribution at the electrode surface which is induced by the additional Helmholtz potential representing the ionic counter plane at the position of the specific atom. The resonant x-ray diffraction spectra are calculated using the FDMNES code. Its ab initio DFT approach uses a free

shape potential allowing the adding of the Helmholtz barrier potential described above. The resonant form factors, giving finally the intensity of the reflections, depend on the local electronic structure around the resonantly excited atoms. The code can thus deliver at the same time and with the same model, for example with or without the Helmholtz potential, the projected density of states (pDOS) on the atoms and the Crystal Orbital Overlap Population (COOP).[41] The COOP is a direct measure of the covalency between 2 neighboring atoms. It corresponds to the integral over space of the product of 2 orbitals of the 2 atoms. Its unit is as for the pDOS, the number of electrons per energy unit. Importantly its sign reveals the bonding (>0) or antibonding (<0) character of the bond. Results on the COOP and pDOS are analyzed in the next sections.

2.2 Experimental details

X-ray measurements. The resonant x-ray scattering experiments were performed at XMaS (BM28), the UK-CRG beamline at the European Synchrotron Radiation Facility in Grenoble. The samples were aligned using an incident x-ray beam energy below the Cu K-edge (8.979 keV). The Cu(001) crystal was indexed to the conventional fcc unit cell with the (0, 0, L) direction along the surface normal ($a^* = b^* = c^* = 2\pi/a$, with a = 3.615 Å) and aligned with the (0, 0, 2) and (1, 1, 1) bulk Bragg reflections. The energy of the incoming x-ray beam was scanned through the Cu and Br absorption K-edges at 8.919 keV and at 13.474 keV, respectively, while the Q-vector was kept constant at the selected point in reciprocal space. A 4-circle diffraction geometry[39, 42] was used and the spectra were each measured in two different geometries changing the polarization of the incoming x-ray beam by 90° with respect to the surface normal to allow to distinguish charge rearrangement parallel and perpendicular to the surface normal. The change in polarization was achieved by physically rotating the sample by 90° while the polarization of the x-rays was kept constant. In the vertical geometry the Q-vector is perpendicular to the polarization of the x-ray beam and at low L parallel to the surface normal. In the horizontal geometry the Q-vector is parallel to the polarization of the beam and at low L perpendicular to the surface normal.[43]

The intensity of the elastically diffracted x-rays was recorded using a Vortex® x-ray detector. This detector has sufficient energy resolution to enable separation of the elastic and the fluorescent x-ray signal from the copper substrate and record both in parallel. The derivative of the recorded fluorescence together with the EXAFS features of the fluorescence was used to define the position of the Cu K-edge and allow exact alignment of the energy spectra measured in the two different geometries. At each particular reciprocal lattice position where energy scans were performed, a background signal was measured by rotating the sample about its surface normal (by ~0.5°) and repeating the energy scan. Each set of scans was repeated at least once to allow for averaging and to acquire sufficiently precise counting statistics.

Sample Preparation and Setup. The Cu(001) single-crystal sample (Mateck, 99.999%, 10 mm diameter, miscut <0.1°) was prepared prior to the experiments by electropolishing in 70% orthophosphoric acid. The sample was covered by a droplet of milli-Q water and mounted into the electrochemical thin layer x-ray cell.[44-46]

In all experiments 10 mM $HClO_4$ + 10 mM KBr solution was prepared from 99.999% trace metals basis KBr (Aldrich) and 99.999% trace metals basis 70% perchloric acid (Aldrich) electrolyte. Perchloric acid was chosen to keep an acidic pH to stop the formation of surface oxide as perchlorate is strongly solvated and thus does not specifically adsorb on the surface.[47] All potentials were measured versus a Ag/AgCl (3 M KCl) reference electrode. The measurements of the x-ray resonant data were performed at OCP (-0.08V versus Ag/AgCl). At this potential the electrode is covered by a full monolayer of bromide. We chose this potential to avoid any possible reference electrode potential shifts as the collection of the full data set took several days. In all measurements, the outer chamber of the x-ray cell was continuously purged with nitrogen to protect the electrode surface from oxygen.

3. Results and discussion

The experimental diffraction spectra obtained at specific points in reciprocal space at the Cu K-edge (8.979 keV) are presented in Figure 2 (a-d). Fig 2 (e-g) shows the calculated electron densities of the empty p-orbital states for the 1st two Cu atomic layers (specifically the Cu atoms labelled in Figure 1) calculated both with and without the presence of the counter ions included through the form of the Helmholtz potential. The structural parameters for the Br adatoms and Cu substrate atoms are based on a previous in-situ surface x-ray diffraction study of the Br-Cu(001) -c(2x2) system. [48] As can be seen, the inclusion of the counter ions only affects the density of states of the outermost layer, Cu_1. We have modelled the Br-Cu(001)–c(2x2) interface both with and without the presence of the potential representing the Helmholtz layer. For the choice of the parameters we have taken a distance, z_0, of 1.9 Å above the Br adlayer which corresponds to 3.4 Å above the first Cu(001) atomic layer. The potential maximum coming from the electrostatic potential due to cation layering above the adsorbed bromine is 18 eV. The width of the potential has been taken as ΔH=2 Å, which corresponds to the potential of a charge distribution with a Gaussian profile along the surface normal with σ=0.4 Å and thus a FWHM of 0.94 Å. Note that the surface atoms are affected only by the tail of the potential distribution, thus small changes in the parameters will not have a large effect. Figure 1 depicts the potential as used to model the data with respect to the atomic positions of the Cu(001)-Br surface. The structural ion layering parameters used in this study to give a good agreement with the experimental data are close to ion ordering parameters found previously.[14, 49-50] Cation-substrate distances were found to be of the order of 2-3 Å for an adsorbate-free aqueous-mica interface and of the order of ~4 Å for an adsorbate-free Ag(111) surface in aqueous solution.[14, 31] In the presence of adsorbed hydroxyl anions the cation layer was found to be stabilized closer to the Ag(111) surface at a distance of ~3.6 Å. [14]

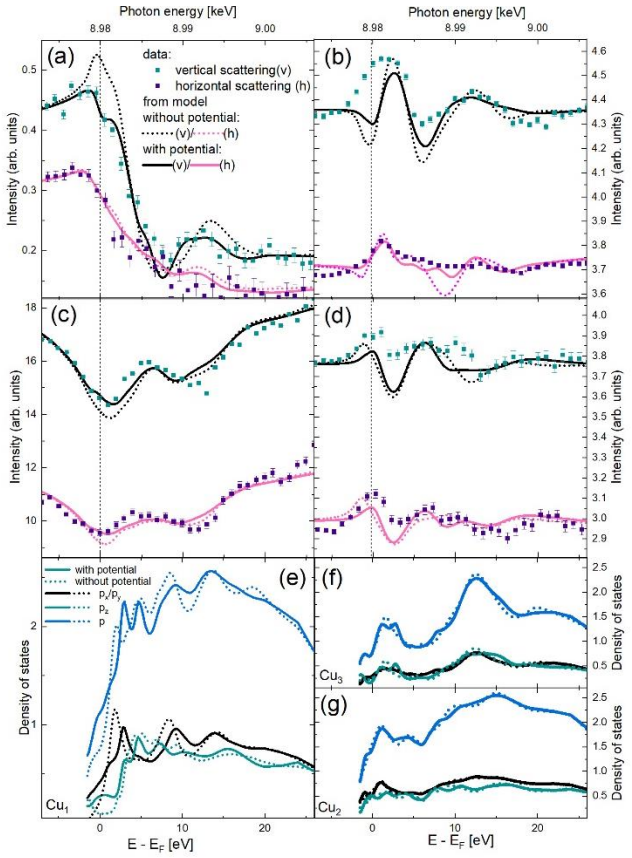

Figure 2. The spectra at different points in reciprocal space (a) (1 1 0.2), (b) (0 1 0.2), (c) (1 1 0.8) and (d) (0 1 0.7) measured in horizontal and vertical polarization mode are shown together with the modelled data obtained both with (solid line) and without (dotted line) applying an additional potential of 18 eV at a distance of 1.9 Å as further specified in the text. Error bars on the measured intensity have been obtained as the square-root of the measured counts in the detector. The position of the Cu K-edge is indicated by a vertical dashed line. The changes in the empty states of the electron density of the 4p-orbitals, which are probed by exciting the Cu K electrons in the Cu atoms in the 1st two atomic layers Cu_1 (e), Cu_2 (f) and Cu_3 (g) are shown to illustrate the changes induced in the spectra. The energy is indicated as the photon energy (against which the data is measured) and as $E-E_F$, with E_F the Fermi energy, for the density of states. The scales are aligned to each other to allow for comparison.

Molecular Dynamics simulations have been able to give a concrete value for the electrostatic potential induced by ion ordering close to a charged interface. A potential of the order of 6 eV has been obtained for a water layer adsorbed close to a Pt(111) surface.[51-52] In this study we need a larger value to reproduce the experimental data than the one obtained in the above-mentioned study. These values are however not unreasonable as we do consider the case of a specifically adsorbed anion layer for which it is not unreasonable to consider a remaining partial charge on the adsorbate in comparison to a potential induced by the dipole moment of adsorbed water. In addition, for the halide covered copper surface the potential at which the data was measured corresponds to a shift of 1.1 V in potential compared to the work function of a halide covered Cu(001) surface in UHV.[53-54] The water layer on Pt(111) was found to induce a lower shift of 0.55 V [51] thus supporting a lower potential due a less ordered charge layer on the solution side of the interface.

The calculated spectra at the points in reciprocal space for which experimental data was recorded, both with and without including the potential representing the counter cations at the interphase, are shown in Figure 2 (a-d). The spectra recorded at the most surface sensitive position, (1 1 0.2), are shown in Figure 2 a. The features of the energy spectra are better reproduced considering the counter ions/Helmholtz layer and the change observed are associated with a modified bonding and shift of the electron density and surface dipole moment as will be discussed below. The (0 1 0.2) and (0 1 0.7) positions (Figure 2b and d, respectively) are sensitive to atoms with the symmetry of the c(2x2) Br adlayer and thus, for the case of the Cu K-edge, have contributions from the second atomic Cu layer only (atoms Cu_2 and Cu_3 in Figure 1). The differences between the intensity modelled with and without including the Helmholtz layer are not as pronounced as for the (1 1 0.2) position, though the near edge structure is slightly better reproduced. To compare the goodness of fit of the model to the experimental data, a distance reliability factor R_1 and a confidence factor D_1 were used.[55-56] The inclusion of the Helmholtz potential in the calculations leads to a reduction in the R_1 and D_1 values from .0012 to .00069 and from 1.096 to 0.925 respectively. These are the values obtained for the entire data set, a breakdown of the R_1 and D_1 values for the individual spectra is presented in the supplementary information in table SI1. The results can be better understood by plotting the calculated electron densities associated with each atom and orbital as shown in Figure 3 for the case with and without the presence of the Helmholtz potential. For the Br adatom, a clear shift to lower energies of the p_z-orbitals combined with a more defined energy range is observed. In addition to the energy spectra at the Cu K-edge, the energy spectra measured at the (0 1 0.2) position, while scanning the energy through Br K-edge, are shown in the supplementary information, Figure SI1.

Localized energy states of the s electrons are also observed in the same lower energy ranges for the 1st two Cu atomic layers. This indicates formation of a stronger bond through orbital overlap, with the charge mostly residing on the Br adatoms. This result is further supported by the COOP which is shown in the supplementary information, Figure S2. The localized energy state at -9 eV with contributions mostly from the Br p- and Cu s-orbitals can be observed. Interestingly sharpening of the energy states can be observed down to the second atomic layer. As discussed previously[57] the assignment of electronic charge belonging to specific atoms is difficult. To distinguish between the amount of charge belonging to the metal and to the adsorbing species is impossible as the charge assigned to a specific atom depends on the area selected for the integration of the electronic density around each atom. Therefore, we only quantitatively discuss the changes in the electron densities and try to further the discussion around charge redistribution by considering differences in charge density maps and potential, as the differences do not rely on a specific radius selected to obtain atomic electron densities. The effect of the electrochemical potential on the electron distribution at the interface is shown in Figure 4, in which the difference of the electron density $\Delta\rho = \rho_2 - \rho_1$ with (ρ_2) and without (ρ_1) the Helmholtz potential is shown along (a) the <100> and (b) the <110> directions (bulk

coordinates) through the Br adsorbate atom. The charge distribution at the atoms has been altered, not only by adding or subtracting charges, thus resulting in simply a charged atom, but by a rearrangement of the electron densities at different distances from the center of the atom. The Br atom shows an additional negative charge which is concentrated towards the center and in an additional sphere around the atom, whereas in between these spheres a slight positive charge can be seen. The Cu atoms close to the surface show an additional positive charge close to the center and in a sphere ~0.5 Å from the center, whereas the space in between these two positive charge accumulations is slightly negatively charged. This can be understood in terms of a redistribution of the charges between the orbitals and a possible hybridization of the orbitals due to a change in the bonding between the atoms. Note that the electron density as shown in Figure 4 is deduced from the contribution of the atomic orbitals only. To estimate the effect of hybridization and of the associated charge rearrangement, the COOP between the different atoms was integrated up to the Fermi level; the difference with and without applying a Helmholtz potential indicates the shift in the charge arrangement in the free electrons (s and p orbitals) due to bond formation and orbital overlap. This is indicated schematically by the '+' and '-' signs in Figure 4. The modification of the potential energy V_r due to the rearrangement of the electron density is also shown in Figure 4 using a different color scheme (green/grey).

From both the change in the electron density rearrangement and the potential a change in the surface dipole moment can be deduced, with a slightly increased negative charge towards the Br adsorbates. Interestingly the origin of the change in the dipole moment does not lie, as might be expected, between the Br adsorbate and the first Cu atomic layer but is actually in the first Cu atomic layer. The origin of the charge modification thus is between the Br-adsorbate and the 2nd Cu atomic layer. These effects explain the buckling of the 2nd Cu atomic layer[53] which can, with the origin of the dipole moment on the 1st Cu atomic layer, be understood as being due to local Friedel oscillations induced by the Br ad-atoms. It is apparent that the simple approximation of a metal electrode with the jellium model is invalid at least when specific adsorption occurs. The first atomic layers of the metal electrode have to be treated differently from the bulk atoms due to the interaction of the surface atoms with ions in solution and subsequent adsorbate formation. The position of the surface or interface can be assumed as the position of the surface dipole moment (Friedel oscillations can induce additional smaller dipole moments further into the substrate). With the dipole surface moment shifting into the metal electrode, the 1st atomic layer cannot clearly be assigned as part of the substrate or of the electrolyte anymore. This may sound counterintuitive from the perspective of traditional surface science but could well help to explain several aspects of electrochemical processes such as corrosion, electrodeposition, the occurrence of underpotential deposition and the stability of catalysts undergoing electrochemical reactions.

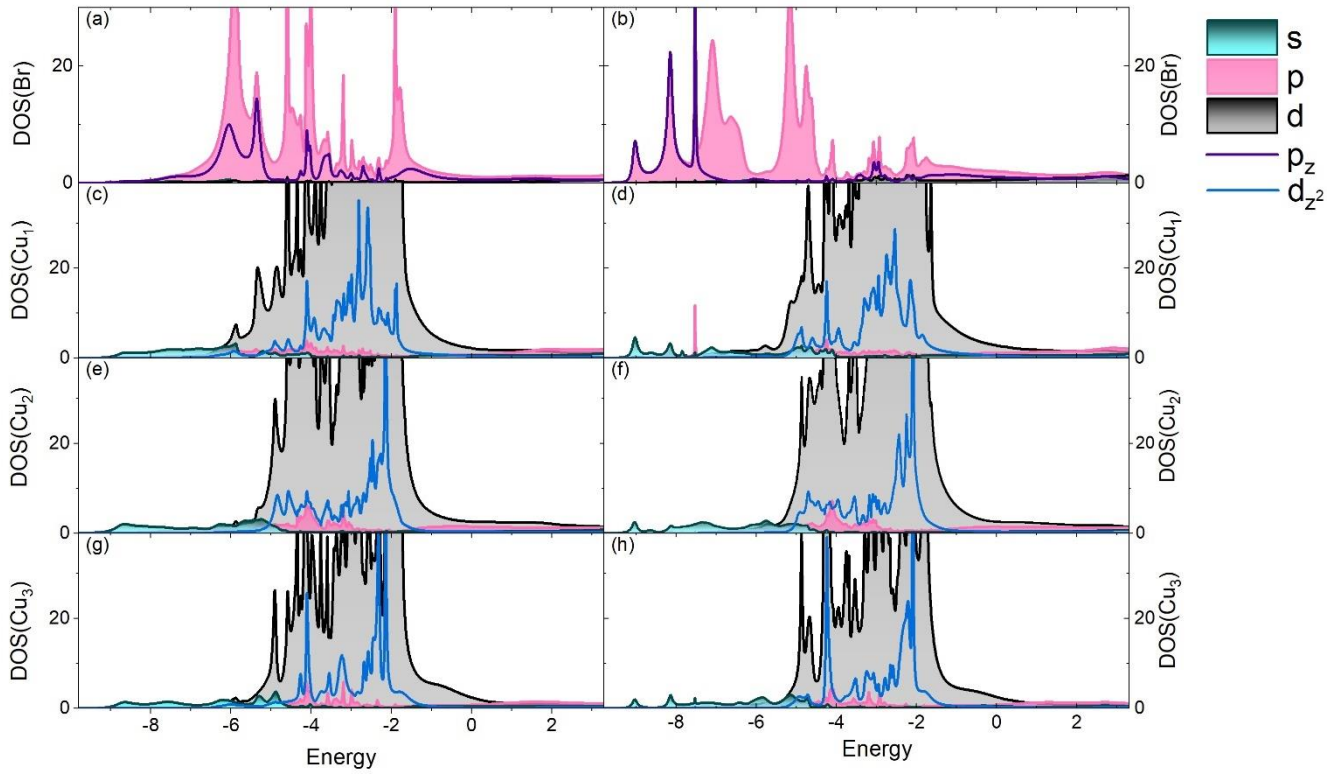

Figure 3. The s-,p-, and d-electron densities obtained by modelling the resonant data without (a,c,e,g) and with an applied potential of 18 eV at a distance of 1.9 Å above the Br adsorbate (b,d,f,h) are shown. The z-contribution of the p and d-orbitals are separately shown as a purple and blue line, respectively. The electron densities are shown for (a,b) the Br adsorbate atom, (c,d,) the 1st layer of Cu atoms, (e,f) the 2nd layer Cu atom beneath an empty hollow site, (g,h) the 2nd layer Cu atom beneath an adsorbed Br atom.

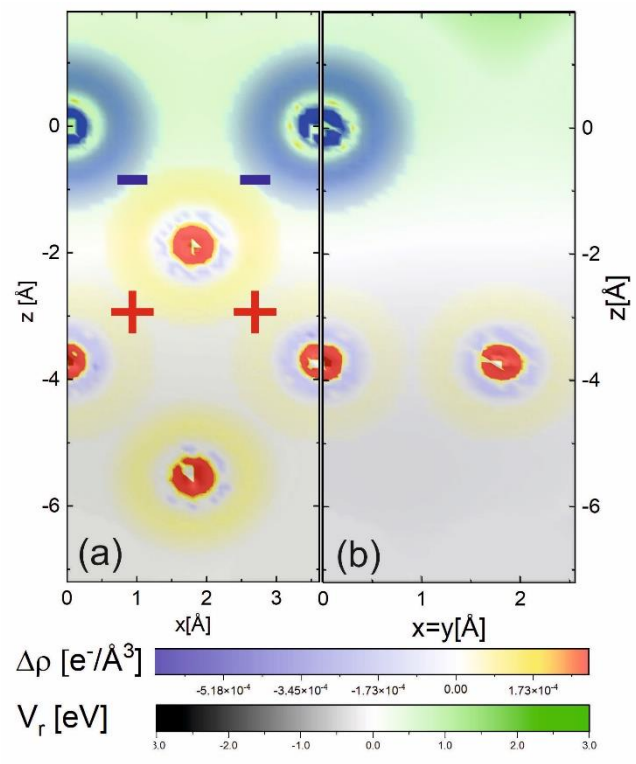

Figure 4. Map of the difference in electron density Δρ and in the potential energy V_r induced by the applied Helmholtz potential and without an applied potential are shown. (a) Shows a cut along the [100] (x) direction (bulk coordinates) through the Br adsorbate. The Br adsorbate atoms and the second copper layer are visible. The '+' and '-' indicate the additional charge rearrangement from the hybridization of the orbitals obtained from the COOP. (b) Shows a cut along the [110] (x=y) direction through the Br atom, the Br adsorbate atom and the 1st copper atoms are visible.

4. Conclusions

In this article we have shown that a combination of in-situ resonant surface x-ray diffraction studies and self-consistent DFT calculations can suitably assess the charge distribution and bonding mechanism at the electrochemical interface for the adsorption of bromide anions onto a single crystal Cu(001) electrode surface. Comparing the experimental and modelled data gives information about the modification of the charge distribution at the interface and the bonding of specific adsorbates in the presence of a Helmholtz potential. A charge reorganization within the atoms at the interface was observed rather than a charge shift in between atoms. In addition, the dipole surface moment shifts into the metal electrode. With a charge modification found down to the second metallic layer, the results imply that it is important to consider the detailed charge distribution in the metal electrode in the modeling of electrochemical reactions.

AUTHOR INFORMATION

Corresponding Author

* Oliver Lodge Laboratory, Department of Physics, University of Liverpool, Liverpool L69 72E, UK
E-mail: grunder @liverpool.ac.uk

Author Contributions

Y.G., C.A.L. and P.T. conceived the project, designed and performed experiments. Y.G. Y.J and Y.S.O discussed the idea for modelling the data. Y.J. wrote and modified the FDMNES code for simulation of the data. The manuscript was written through contributions of all authors. All authors have given approval to the final version of the manuscript.

ACKNOWLEDGMENT

YG thanks the Royal Society for funding through a University Research Fellowship (URF\R\180005) and a research grant (RGF\EA\181030). YG, YJ, YSO and CAL thank the Royal Society for support though an International Exchanges grant (IES\R2\202033). RSXRD measurements were performed on the EPSRC-funded XMaS CRG beamline (EP/S020845/1) at the ESRF, Grenoble, France.

Supporting information available:

Resonant diffraction on the superstructure recorded at the Br K-edge, Orbital overlap between the different atoms (COOP) from 1st principle modelling and the individual changes in the distance reliability factor R_1 and confidence factor D_1 are given.

REFERENCES

1. Krug, K.; Stettner, J.; Magnussen, O. M., In-situ surface x-ray diffraction studies of homoepitaxial electrochemical growth on Au(100). *Physycal Review Letters* **2006,** *96*, 246101.
2. Golks, F.; Grunder, Y.; Drunkler, A.; Roy, J.; Stettner, J.; Zegenhagen, J.; Magnussen, O. M., In situ surface x-ray diffraction studies of the influence of the peg-cl-complex on homoepitaxial electrodeposition on Cu(001). *Journal of the Electrochemical Society* **2013,** *160* (12), D3165-D3170.
3. Golks, F.; Gründer, Y.; Stettner, J.; Krug, K.; Zegenhagen, J.; Magnussen, O. M., In situ surface x-ray diffraction studies of homoepitaxial growth on Cu(001) from aqueous acidic electrolyte. *Surface Science* **2015,** *631*, 112-122.
4. Golks, F.; Stettner, J.; Gründer, Y.; Krug, K.; Zegenhagen, J.; Magnussen, O. M., Anomalous potential dependence in homoepitaxial Cu(001) electrodeposition: An in situ surface x-ray diffraction study. *Physical Review Letters* **2012,** *108* (25), 256101.
5. Hermann, J. M.; Mattausch, Y.; Weiß, A.; Jacob, T.; Kibler, L. A., Enhanced Electrocatalytic Oxidation of Formic Acid on Au(111) in the Presence of Pyridine. *Journal of The Electrochemical Society* **2018,** *165* (15), J3192-J3198.
6. Grunder, Y.; Beane, J.; Kolodziej, A.; Lucas, C. A.; Rodriguez, P., Potential Dependent Structure and Stability of Cu(111) in Neutral Phosphate Electrolyte. *Surfaces* **2019,** *2* (1), 145-158.
7. Kolb, D. M., Reconstruction phenomena at metal-electrolyte interfaces. *Progress in Surface Science* **1996,** *51* (2), 109-173.
8. Kaghazchi, P.; Fantauzzi, D.; Anton, J.; Jacob, T., Nanoscale-faceting of metal surfaces induced by adsorbates. *Physical Chemistry Chemical Physics* **2010,** *12* (31), 8669-8684.
9. Pender, J. P.; Jha, G.; Youn, D. H.; Ziegler, J. M.; Andoni, I.; Choi, E. J.; Heller, A.; Dunn, B. S.; Weiss, P.

S.; Penner, R. M.; Mullins, C. B., Electrode Degradation in Lithium-Ion Batteries. *ACS Nano* **2020,** *14* (2), 1243-1295.
10. Angelucci, C. A.; Souza-Garcia, J.; Feliu, J. M., The role of adsorbates in electrocatalytic systems: An analysis of model systems with single crystals. *Current Opinion in Electrochemistry* **2021,** *26*, 100666.
11. Chen, L.; Dang, J.; Du, J.; Wang, C.; Mo, Y., Hydrogen and Halogen Bonding in Homogeneous External Electric Fields: Modulating the Bond Strengths. *Chemistry – A European Journal* **2021,** *27* (56), 14042-14050.
12. Kong, N.; Guo, J.; Chang, S.; Pan, J.; Wang, J.; Zhou, J.; Liu, J.; Zhou, H.; Pfeffer, F. M.; Liu, J.; Barrow, C. J.; He, J.; Yang, W., Direct Observation of Amide Bond Formation in a Plasmonic Nanocavity Triggered by Single Nanoparticle Collisions. *Journal of the American Chemical Society* **2021,** *143* (26), 9781-9790.
13. Abad, J. M.; Gass, M.; Bleloch, A.; Schiffrin, D. J., Direct electron transfer to a metalloenzyme redox center coordinated to a monolayer-protected cluster. *Journal of the American Chemical Society* **2009,** *131* (29), 10229-10236.
14. Lucas, C. A.; Thompson, P.; Gründer, Y.; Markovic, N. M., The structure of the electrochemical double layer: Ag(111) in alkaline electrolyte. *Electrochemistry Communications* **2011,** *13* (11), 1205-1208.
15. Toney, M. F.; Howard, J. N.; Richer, J.; Borges, G. L.; Gordon, J. G.; Melroy, O. R.; Yee, D.; Sorensen, L. B., Electrochemical deposition of copper on a gold electrode in sulfuric acid: resolution of the interfacial structure. *Phys Rev Lett* **1995,** *75* (24), 4472-4475.
16. Steinrück, H.-G.; Cao, C.; Tsao, Y.; Takacs, C. J.; Konovalov, O.; Vatamanu, J.; Borodin, O.; Toney, M. F., The nanoscale structure of the electrolyte–metal oxide interface. *Energy & Environmental Science* **2018,** *11* (3), 594-602.
17. Zhou, S.; Panse, K. S.; Motevaselian, M. H.; Aluru, N. R.; Zhang, Y., Three-Dimensional Molecular Mapping of Ionic Liquids at Electrified Interfaces. *ACS Nano* **2020,** *14* (12), 17515-17523.
18. Tong, Y.; Lapointe, F.; Thämer, M.; Wolf, M.; Campen, R. K., Hydrophobic Water Probed Experimentally at the Gold Electrode/Aqueous Interface. *Angewandte Chemie International Edition* **2017,** *56* (15), 4211-4214.
19. Letchworth-Weaver, K.; Arias, T. A., Joint density functional theory of the electrode-electrolyte interface: Application to fixed electrode potentials, interfacial capacitances, and potentials of zero charge. *Physical Review B* **2012,** *86* (7), 075140.
20. Schultze, J. W.; Koppitz, F. D., Bond formation in electrosorbates - I Correlation between the electrosorption valency and Pauling's electronegativity for aqueous solutions. *Electrochimica Acta* **1976,** *21*, 327-336.
21. *Comprehensive treatise of electrochemistry. Vol. 1*. Plenum Press: New York, 1980; Vol. 1.
22. Schmickler, W.; Guidelli, R., The partial charge transfer. *Electrochimica Acta* **2014,** *127*, 489-505.
23. Schultze, J. W.; Rolle, D., The partial discharge of electrosorbates and its influence in electrocatalysis. *Can.J.Chem.* **1997,** *75*, 1750-1758.
24. Stoffelsma, C.; Rodriguez, P.; Garcia, G.; Garcia-Araez, N.; Strmcnik, D.; Markovic, N. M.; Koper, M. T., Promotion of the oxidation of carbon monoxide at stepped platinum single-crystal electrodes in alkaline media by lithium and beryllium cations. *J Am Chem Soc* **2010,** *132* (45), 16127-33.
25. Strmcnik, D.; Kodama, K.; van der Vliet, D.; Greeley, J.; Stamenkovic, V. R.; Markovic, N. M., The role of non-covalent interactions in electrocatalytic fuel-cell reactions on platinum. *Nat Chem* **2009,** *1* (6), 466-72.
26. Colic, V.; Pohl, M. D.; Scieszka, D.; Bandarenka, A. S., Influence of the electrolyte composition on the activity and selectivity of electrocatalytic centers. *Catalysis Today* **2016,** *262*, 24-35.
27. Frumkin, A. N., *Z.Phys.Chem.* **1933,** *164A*, 121.
28. Frumkin, A. N., Influence of cation adsorption on the kinetics of electrode processes. *Transactions of the Faraday Society* **1959,** *55* (0), 156-167.
29. Waegele, M. M.; Gunathunge, C. M.; Li, J.; Li, X., How cations affect the electric double layer and the rates and selectivity of electrocatalytic processes. *The Journal of Chemical Physics* **2019,** *151* (16), 160902.
30. Fenter, P.; Sturchio, N. C., Mineral-water interfacial structures revealed by synchrotron X-ray scattering. *Progress in Surface Science* **2005,** *77* (5-8), 171-258.
31. Bourg, I. C.; Lee, S. S.; Fenter, P.; Tournassat, C., Stern Layer Structure and Energetics at Mica–Water Interfaces. *The Journal of Physical Chemistry C* **2017,** *121* (17), 9402-9412.
32. Saveleva, V.; Savinova, E., Insights into electrocatalysis from ambient pressure photoelectron spectroscopy. **2019,** *17*, 79-89.
33. Menzel, A.; Chang, K.-C.; Komanicky, V.; You, H.; Chu, Y. S.; Tolmachev, Y. V.; Rehr, J. J., Resonance anomalous surface X-ray scattering. *Radiation Physics and Chemistry* **2006,** *75* (11), 1651-1660.
34. Menzel, A.; Tolmachev, Y. V.; Chang, K. C.; Komanicky, V.; Chu, Y. S.; Rehr, J. J.; You, H., Polarization-dependent resonant anomalous surface X-ray scattering of CO/Pt(111). *Europhysics Letters (EPL)* **2006,** *74* (6), 1032-1038.
35. Bourke, J. D.; Chantler, C. T.; Joly, Y., FDMX: Extended X-ray absorption fine structure calculations using the finite difference method. *Journal of Synchrotron Radiation* **2016,** *23* (2), 551-559.
36. Bunău, O.; Joly, Y., Self-consistent aspects of x-ray absorption calculations. *Journal of Physics Condensed Matter* **2009,** *21* (34), 345501.
37. Joly, Y.; Abisset, A.; Bailly, A.; De Santis, M.; Fettar, F.; Grenier, S.; Mannix, D.; Ramos, A. Y.; Saint-Lager, M.-C.; Soldo-Olivier, Y.; Tonnerre, J.-M.; Guda, S. A.; Gründer, Y., Simulation of Surface Resonant X-ray Diffraction. *Journal of Chemical Theory and Computation* **2018,** *14* (2), 973-980.
38. Soldo-Olivier, Y.; Sibert, E.; De Santis, M.; Joly, Y.; Gründer, Y., Unraveling the Charge Distribution at the Metal-Electrolyte Interface Coupling in Situ Surface

Resonant X-Ray Diffraction with Ab Initio Calculations. *ACS Catalysis* **2022**, 2375-2380.
39. Grunder, Y.; Lucas, C. A., Probing the charge distribution at the electrochemical interface. *Physical Chemistry Chemical Physics* **2017,** *19* (12), 8416-8422.
40. Joly, Y.; Matteo, S. D.; Bunău, O., Resonant X-ray diffraction: Basic theoretical principles. *European Physical Journal: Special Topics* **2012,** *208* (1), 21-38.
41. Diaz-Lopez, M.; Guda, S. A.; Joly, Y., Crystal Orbital Overlap Population and X-ray Absorption Spectroscopy. *The Journal of Physical Chemistry A* **2020,** *124* (29), 6111-6118.
42. Toney, M. F.; Weisler, D. G., Instrumental effects on measurements of surface X-ray diffraction rods: resolution function and active sample area. *Acta Crystallographica Section A* **1993,** *49* (4), 624-642.
43. Paolasini, L., Resonant and magnetic X-ray diffraction by polarized synchrotron radiation. *JDN* **2014,** *13*, 03002.
44. Gründer, Y.; Thompson, P.; Brownrigg, A.; Darlington, M.; Lucas, C. A., Probing the halide-metal interaction by monolayer metal deposition at the electrochemical interface. *Journal of Physical Chemistry C* **2012,** *116* (10), 6283-6288.
45. Tidswell, I. M.; Markovic, N. M.; Lucas, C. A.; Ross, P. N., In situ x-ray-scattering study of the Au(001) reconstruction in alkaline and acidic electrolytes. *Phys Rev B Condens Matter* **1993,** *47* (24), 16542-16553.
46. Samant, M. G.; Toney, M. F.; Borges, G. L.; Blum, L.; Melroy, O. R., In-situ grazing incidence X-ray diffraction study of electrochemically deposited Pb monolayers on Ag(111). *Surface Science* **1988,** *193* (1-2), L29-L36.
47. Magnussen, O. M., Ordered anion adlayers on metal electrode surfaces. *Chemical Reviews* **2002,** *102* (3), 679-725.
48. Saracino, M.; Broekmann, P.; Gentz, K.; Becker, M.; Keller, H.; Janetzko, F.; Bredow, T.; Wandelt, K.; Dosch, H., Surface relaxation phenomena at electrified interfaces: Revealing adsorbate, potential, and solvent effects by combined x-ray diffraction, STM, and DFT studies. *Physical Review B* **2009,** *79*, 115448.
49. Toney, M. F.; Howard, J. N.; Richer, J.; Borges, G. L.; Gordon, J. G.; Melroy, O. R.; Wiesler, D. G.; Yee, D.; Sorensen, L. B., Voltage-dependent ordering of water molecules at an electrode–electrolyte interface. *Nature* **1994,** *368* (6470), 444-446.
50. Bourg, I. C.; Lee, S. S.; Fenter, P.; Tournassat, C., Stern Layer Structure and Energetics at Mica-Water Interfaces. *Journal of Physical Chemistry C* **2017,** *121* (17), 9402-9412.
51. Sakong, S.; Gross, A., The electric double layer at metal-water interfaces revisited based on a charge polarization scheme. *J Chem Phys* **2018,** *149* (8), 084705.
52. Skulason, E.; Karlberg, G. S.; Rossmeisl, J.; Bligaard, T.; Greeley, J.; Jonsson, H.; Norskov, J. K., Density functional theory calculations for the hydrogen evolution reaction in an electrochemical double layer on the Pt(111) electrode. *Phys Chem Chem Phys* **2007,** *9* (25), 3241-50.
53. Gründer, Y.; Kaminski, D.; Golks, F.; Krug, K.; Stettner, J.; Magnussen, O. M.; Franke, A.; Stremme, J.; Pehlke, E., Reversal of chloride-induced Cu(001) subsurface buckling in the electrochemical environment: An in situ surface x-ray diffraction and density functional theory study. *Physical Review B - Condensed Matter and Materials Physics* **2010,** *81* (17), 174114.
54. Trasatti, S., Structuring of the solvent at metal/solution interfaces and components of the electrode potential. *J.Electroanal.Chem.* **1983,** *150*, 1-15.
55. Joly, Y.; Lorenzo, J. E.; Nazarenko, E.; Hodeau, J. L.; Mannix, D.; Marin, C., Low-temperature structure of magnetite studied using resonant x-ray scattering. *Physical Review B - Condensed Matter and Materials Physics* **2008,** *78* (13), 134110.
56. De Santis, M.; Bailly, A.; Coates, I.; Grenier, S.; Heckmann, O.; Hricovini, K.; Joly, Y.; Langlais, V.; Ramos, A. Y.; Richter, C.; Torrelles, X.; Garaudee, S.; Geaymond, O.; Ulrich, O., Epitaxial growth and structure of cobalt ferrite thin films with large inversion parameter on Ag(001). *Acta Crystallographica Section B* **2019,** *75* (1), 8-17.
57. Ávila, M.; Juárez, M. F.; Santos, E., Role of the Partial Charge Transfer on the Chloride Adlayers on Au(100). *ChemElectroChem* **2020,** *7* (20), 4269-4282.

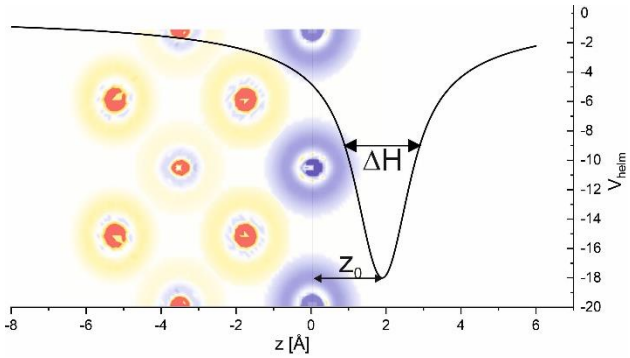

For table of contents only

Charge Reorganization at the Adsorbate covered Electrode Surface probed through in-situ resonant x-ray Diffraction combined with ab-initio Modelling

Yvonne Grunder,[‡,] * Christopher A. Lucas,[‡] Paul B.J. Thompson,[‡,†] Yves Joly,[§] Yvonne Soldo-Olivier[§]

[‡] Oliver Lodge Laboratory, Department of Physics, University of Liverpool, Liverpool L69 72E, UK

[†] XMaS Beamline, European Synchrotron Radiation Facility, F-38043 Grenoble, France

[§] Université Grenoble Alpes, CNRS, Institut Néel, 38042 Grenoble, France

Supporting information

(1) Experimental results on the Br-Kedge

In addition to the energy spectra at the Cu K-edge, the energy spectra measured at the (0 1 0.2) position, while scanning the energy through Br K-edge, were measured and are shown in Figure SI1. With the bromine adatoms only occupying one symmetric site, the spectra observed at the Br K-edge resemble typical adsorption spectra.

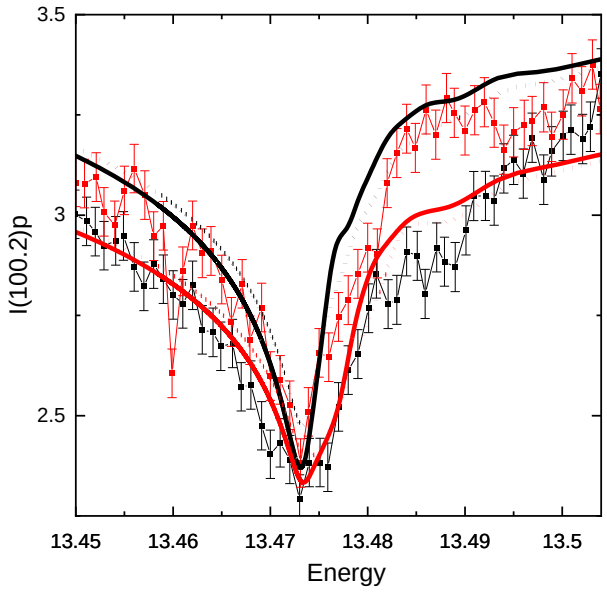

Figure SI1: *The spectra at the (0 1 0.2) position on the c(2x2) superstructure rod as measured in horizontal and vertical polarisation around the Br K-edge are shown together with the modelled data obtained without applying an additional potential (dotted line) and with applying an additional potential of 18 eV at a distance of 1.9 Å (solid line) as further specified in the text.*

(2) Orbital overlap between the different atoms (COOP) from 1st principle modelling

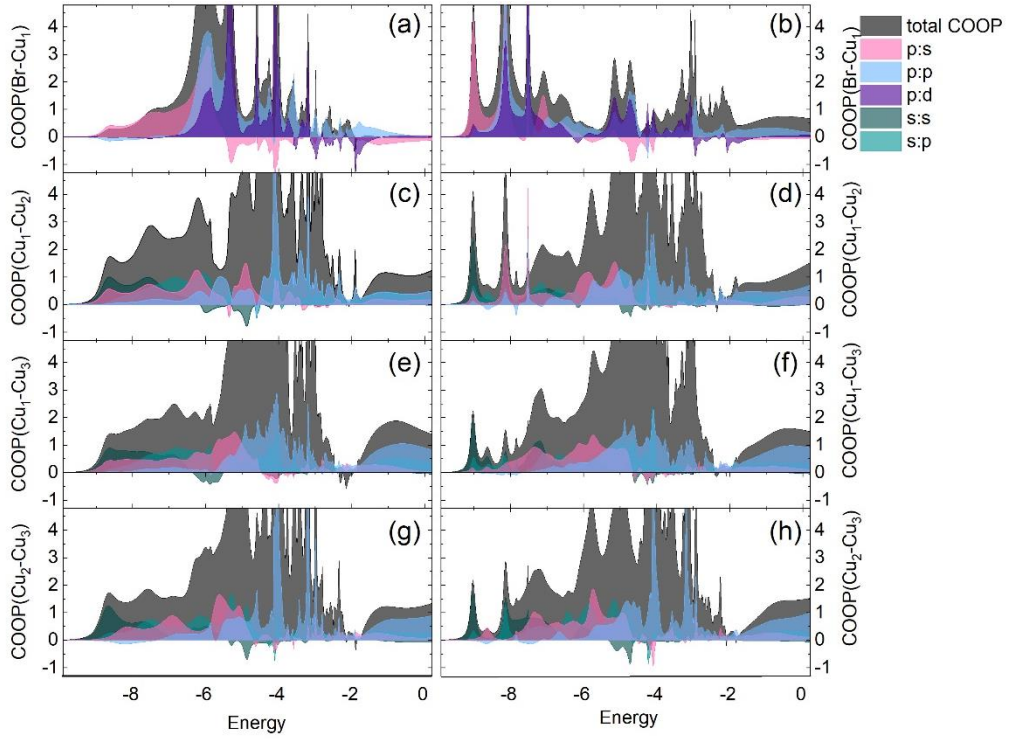

Figure SI2: *The overlap of the orbitals between the different atoms (COOP) for (a,b) the Br on copper in the 1st layer, (c,d) 1st layer copper and 2nd layer copper atom beneath the bromide adsorbate, (e,f) 1st layer copper and 2nd layer copper atom beneath an adsorbate free hollow site and (g,h) between the two copper atoms in the second layer as obtained from the model without (a,c,e,g) and with a potential of 18 eV at a distance of 1.9 Å above the Br adsorbate (b,d,f,h) applied.*

		with potential		without potential		Difference Δ	
position	**polarisation**	**D1**	**Rx**	**D1**	**Rx**	**Δ D1**	**Δ R1**
0 1 0.2	horizontal	0.252	0.0001	0.295	0.0002	0.043	0.0001
0 1 0.2	vertical	0.336	0.0002	0.440	0.0004	0.104	0.0002
0 1 0.7	horizontal	0.486	0.0004	0.456	0.0005	-0.030	0.0001
0 1 0.7	vertical	0.322	0.0002	0.319	0.0003	-0.002	0.0001
1 1 0.2	horizontal	1.756	0.0046	2.602	0.0121	0.846	0.0074
1 1 0.2	vertical	2.257	0.0060	2.394	0.0070	0.136	0.0010
1 1 0.8	horizontal	0.875	0.0010	1.069	0.0016	0.194	0.0006
1 1 0.8	vertical	1.116	0.0015	1.190	0.0016	0.074	0.0001

Table SI1: *The individual changes in the R_1 and D_1 values for each position in reciprocal space are shown. The last two columns show the difference subtracting the values obtained with potential from the ones obtained without potential. It can be seen that overall a better agreement between the data and the model is achieved for the positions (0 1 0.2), (1 1 0.2) and (1 1 0.8). Only the position at (0 1 0.7) does not show an improvement however the changes in D1 and R1 are much smaller than observed for the other positions.*